Formulation of Low-Order Dominant Poles for Y-matrix of Interconnects

Qinwei Xu and Pinaki Mazumder *
EECS Dept., University of Michigan, Ann Arbor, MI 48109-2122
Email: {qwxu,mazum}@eecs.umich.edu

Abstract

This paper presents an efficient approach to compute the dominant poles for the reduced-order admittance (Y parameter) matrix of lossy interconnects. Using the global approximation technique, the efficient frameworks are constructed to transform the frequency-domain Telegrapher's equations into compact linear algebraic equations. The dominant poles and residues can be extracted by directly solving the linear equations. The closed-form formulas are derived to compute the low-order dominant poles. Due to high accuracy of the global approximation, the extracted poles can accurately represent the exact admittance matrices in a wide frequency range. By using the recursive convolution technique, the pole-residue models can be represented by companion models, which have linear complexity with respect to the computational time. The presented modeling approaches are shown to preserve passivity. Numerical experiments of transient simulation show that the presented modeling approaches lead to higher efficiency, while maintaining comparable accuracy.

1 Introduction

For the design of giga-hertz and multimillion-transistor VLSI systems, accurate and efficient interconnect modeling has assumed an increasingly important status, since long interconnects in such designs dominate the signal integrity, speed of operation, silicon real estate as well as the power dissipation of the integrated circuits. Long metal interconnects in such high-speed ICs are now treated as lossy transmission lines with distributed RLC parameters and reduced order models are generally employed for efficient circuit simulation. Asymptotic Waveform Evaluation (AWE) is the well-known method to obtain the reduced-order models of linear networks [1, 2]. It directly calculates the Laplace domain moments of the port characteristics and obtain the Padé approximation by moment-matching technique. The poles/residues of the rational approximation are used to describe the reduced-order macromodel. The algorithms of multipoint moment-matching, like Complex Frequency Hopping (CFH), were developed for indirect reduced-order modeling [3]. Krylov subspace techniques and congruence transformations have been successfully applied in passive model order reduction [4]. An extended technique based on Arnoldi's method with congruence transformations is presented in the literature [5], in which the PRIMA algorithm was demonstrated as an effective approach to develop passive reduced-order models.

For individual interconnect modeling, most effort to develop reduced-order models follow a two-step approach: direct discretization of the interconnect and the follow-up order reduction. The first step generally selects many grid points along the transmission line, which results in a large linear system with a considerably high order. The second step then applies the afore-mentioned reduction algorithms to reduce the high order system to a small one with a reasonably low order. Despite the simplicity of direct discretization and the applicability of the reduction algorithms, the two-step approach has, however, the disadvantage of higher complexity. Furthermore, the reduced order models by using this approach may unnecessarily include some redundant poles, which hinders the modeling efficiency [6].

For efficient circuit simulation using the modified nodal approach (MNA), the admittance matrix (Y parameter) modeling is preferred, because the current variables can be avoided in the list of MNA state variables [7]. On the other hand, the admittance matrices gain advantage over the transfer functions in the sense that the Y-matrix can completely represent a device while the transfer function cannot. The Y parameter modeling is independent of source/load impedances, while the transfer function modeling has to adjust the gain of their responses for the finite load. Although Y-matrix is preferred, the frequency-domain analytical representations of Y parameters are composed of transcendental functions, which cannot be transformed into the time-domain, and therefore cannot directly incorporated into the time-domain simulator. As a potential solution, the AWE technique can be used to obtain the rational approximation of Y parameters [8], but this method suffers from complex moment-matching process (Padé approximation) and potential instability.

In this paper, the approximation frameworks are constructed for interconnect modeling by using the global approximation. The frameworks lead to reduced-order models represented by the admittance matrices, which capture the low-order dominant poles of Y parameter of interconnects. The contributions of this paper include: (a) constructing the frameworks of voltage difference and current difference by using the global approximations, (b) calculating the dominant poles of Y parameter from the approximation frameworks and deriving the

* This work was partially supported by ONR grant under the IMS Program.

closed-form formula for computing the low-order dominant poles, and (c) deriving the companion models from the calculated poles/residues. The organization of this paper is as follows. In Section 2, the admittance matrix of interconnect modeling is reviewed, the global approximation mechanisms of voltage difference and current difference are introduced, and the closed-form formula for computing the first 3 and first 5 dominant poles of Y matrix of interconnects are derived. The companion model based on the pole-residue model is obtained, and the passivity of presented modeling approaches are examined in Section 3. The numerical examples are then shown in Section 4 and the conclusions are made in Section 5.

2 Y matrix with dominant poles

For simplicity and without loss of generality, we study the single interconnect first. Assume that the interconnect has the normalized length stretching from 0 to 1 along the x axis (Fig. 1(a)). Let R, L, and C represent the normalized distributed per-unit-length (PUL) resistance, inductance, and capacitance of the line, respectively. The s-domain Telegrapher's equations can be written as:

$$\begin{aligned} V'(x,s) &= -Z(s)I(x,s) \\ I'(x,s) &= -Y(s)V(x,s). \end{aligned} \tag{1}$$

where $V(x,s)$ and $I(x,s)$ are distributed voltage and distributed current, respectively; The sign $'$ denotes the derivative with respect to x; and

$$\begin{aligned} Z(s) &= sL + R \\ Y(s) &= sC. \end{aligned}$$

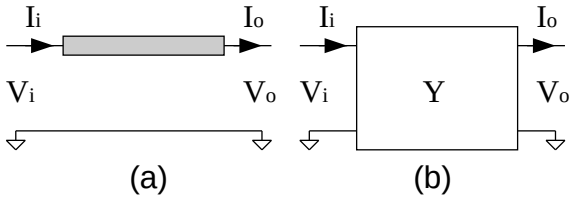

Figure 1: Single transmission line and its two-port representation

The single interconnect can be considered as a two-port network as in Fig. 1(b). For convenience, the port variables are selected as shown. Therefore, in the admittance matrix model, the current variables are I_i and $-I_o$ and the independent voltage variables are V_i and V_o. Under these definitions, the interconnect can be represented by Y parameters:

$$\begin{bmatrix} I_i \\ -I_o \end{bmatrix} = \begin{bmatrix} Y_{11}(s) & Y_{12}(s) \\ Y_{21}(s) & Y_{22}(s) \end{bmatrix} \begin{bmatrix} V_i \\ V_o \end{bmatrix} \tag{2}$$

where

$$\begin{aligned} Y_{11}(s) = Y_{22}(s) &= Y_0(s)\cosh(\gamma)/\sinh(\gamma) \\ Y_{12}(s) = Y_{21}(s) &= -Y_0(s)/\sinh(\gamma) \end{aligned} \tag{3}$$

and

$$Y_0(s) = \sqrt{Y(s)/Z(s)} \tag{4}$$

$$\gamma = \sqrt{Y(s)Z(s)} \tag{5}$$

are characteristic impedance and normalized propagation constant, respectively. Since that each of the entries of Eqn. 3 contains poles and zeros, applying Padé approximation to the entries may give a better low-order model. As shown in [7], the time-domain counterparts of Y parameters show ringing. Because circuit ringing creates complex pole pair(s) in the transfer function, at least one pair of conjugate complex poles is needed to represent the Y parameters with reasonable precision. Applying Padé approximation/AWE to each entry of Y parameter can obtain the poles. However, the moment-generation and moment-matching in AWE are considerably complex and Padé approximation may result in instability; Simple and reliable approaches are thus desired.

2.1 Global approximation frames

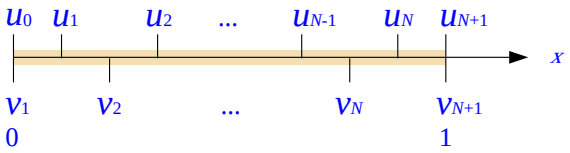

Figure 2: Approximation framework.

Assuming that the distributed voltage and distributed current are smooth, they can be approximately represented by the following functions

$$\begin{aligned} V(x,s) &= \textstyle\sum_{i=0}^{n} c_i x^i V(s) \\ I(x,s) &= \textstyle\sum_{i=0}^{m} d_i x^i I(s) \end{aligned} \tag{6}$$

where the orders n and m may vary with respect to the different requirements of approximation. As shown in Fig. 2, segmenting the interconnect into $2N$ sections, each section has the length of $h = 0.5/N$. Defining the voltage grid set:

$$\{u_0 = 0, u_i = (2i-1)h, i = 1, \ldots, N, u_{N+1} = 1\}, \tag{7}$$

and the current grid set:

$$\{v_i = 2(i-1)h, i = 1, \ldots, N+1\}, \tag{8}$$

the approximation frameworks for voltage difference and current difference are constructed, respectively:

$$V(u_{k+1},s) - V(u_k,s) = \sum_{j=1}^{N+1} a_{kj} V'(v_j,s) \tag{9}$$

$$I(v_{k+1},s) - I(v_k,s) = \sum_{j=1}^{N} b_{kj} I'(u_j,s), \tag{10}$$

where a_{ij}'s and b_{ij}'s are the coefficients to be determined by using the generalized Galerkin's method [9], with the power function set $f(x) = \{1, x, x^2 \ldots\}$ (from Eqn. 6) being test functions. For each k, we substitute an appropriate number of test functions from $f(x) = 1$ to $f(x) = x^n$ into Eqn. 9, then a set of $(N+1) \times (N+1)$ linear equations are obtained, with $\{a_{k1}, a_{k2}, \ldots, a_{k(N+1)}\}$ being the unknowns. The coefficients can be obtained by solving these linear equations. The coefficients $\{b_{k1}, b_{k2}, \ldots, b_{kN}\}$ can be calculated by the similar way.

For simplicity, denote $V_i = V(u_i, x), i = 0, \ldots, N+1$ and $I_i = I(v_i, x), i = 1, \ldots, N$. From Eqns. 9, 10 and Eqn. 1, we obtain the voltage difference and current difference approximations, respectively:

$$\begin{bmatrix} V_1 - V_0 \\ \vdots \\ V_{N+1} - V_N \end{bmatrix} = -Z(s)A \begin{bmatrix} I_1 \\ \vdots \\ I_{N+1} \end{bmatrix} \tag{11}$$

$$\begin{bmatrix} I_2 - I_1 \\ \vdots \\ I_{N+1} - I_N \end{bmatrix} = -Y(s)B \begin{bmatrix} V_1 \\ \vdots \\ V_N \end{bmatrix} \tag{12}$$

where

$$A = \begin{bmatrix} a_{11} & \cdots & a_{1(N+1)} \\ & \ddots & \\ a_{(N+1)1} & \cdots & a_{(N+1)(N+1)} \end{bmatrix} \tag{13}$$

$$B = \begin{bmatrix} b_{11} & \cdots & b_{1N} \\ & \ddots & \\ b_{N1} & \cdots & b_{NN} \end{bmatrix} \tag{14}$$

The approximations in Eqns. 11 and 12 are global, because the voltage or current difference is represented by the values distributed in the entire domain. The local approximations like FD method use up to second order polynomials to determine the coefficients, leading to the accuracy of at best second order. The global approximations in Eqns. 11 and 12 use up to $(N+1)$-th order power function to determine the approximation framework, which achieves the best accuracy of N-th order in this case.

Assuming that V_0 and V_{N+1} are two independent voltage sources, then the modified node admittance (MNA) equation of this model can be expressed as:

$$\begin{bmatrix} B & P \\ -P^T & A \end{bmatrix} \begin{bmatrix} V \\ I \end{bmatrix} = D \begin{bmatrix} V_0 \\ V_{N+1} \end{bmatrix} \tag{15}$$

where

$$V = [V_1 \ldots V_N]^T \tag{16}$$

$$I = [I_1 \ldots I_{N+1}]^T \tag{17}$$

$$P = \begin{bmatrix} -1 & 1 & & \\ & \ddots & \ddots & \\ & & -1 & 1 \end{bmatrix} \tag{18}$$

$$D = \begin{bmatrix} 0 & \ldots & 0 & 1 & \ldots & 0 \\ 0 & \ldots & 0 & 0 & \ldots & -1 \end{bmatrix}^T \tag{19}$$

The Y-matrix is therefore obtained,

$$Y = D^T \begin{bmatrix} B & P \\ -P^T & A \end{bmatrix}^{-1} D \tag{20}$$

If these matrices A and B have very large dimensions, the computation of inverse matrix will become very difficult. However, the dimension of the matrices to compute the most dominant poles are generally small. As shown in the numerical experiments, $N \leq 3$ can already give considerably accurate results in practical interconnect modeling. Next we will study the simplest cases.

2.2 3rd order poles

If the value of N in Eqns. 9 and 10 is selected to be 1, then along the line, three grid points are selected: $x_0 = 0$, $x_1 = 1/2$ and $x_2 = 1$. Following the process introduced above, we take three voltage variables $V_0 = V(x_0, s)$, $V_1 = V(x_1, s)$ and $V_2 = V(x_2, s)$, and two current variables $I_1 = I(x_0, s)$ and $I_2 = I(x_2, s)$ at the grid points. By applying the global approximation to compute the current and voltage difference, we obtain the following approximation frames:

$$\begin{bmatrix} V(x_1, s) - V(x_0, s) \\ V(x_2, s) - V(x_1, s) \end{bmatrix} = \begin{bmatrix} a_{11} & a_{12} \\ a_{21} & a_{22} \end{bmatrix} \begin{bmatrix} V'(x_0, s) \\ V'(x_2, s) \end{bmatrix} \tag{21}$$

and

$$I(x_2) - I(x_1) = bI'(x_1) \tag{22}$$

where a_{11}, a_{12}, a_{21}, a_{22} and b are coefficients to be determined by using fitting functions. Using the generalized Galerkin's method [9], we choose $V(x, s) = \{1, x, x^2\}$ as fitting functions to determine a_{11}, a_{12} in the first line of Eqn. 21, then it follows:

$$x_1 - x_0 = a_{11}x'|_{x_0} + a_{12}x'|_{x_2} \tag{23}$$

$$x_1^2 - x_0^2 = a_{11}(x^2)'|_{x_0} + a_{12}(x^2)'|_{x_2} \tag{24}$$

which results in $a_{11} = 3/8$ and $a_{12} = 1/8$. Doing the same operations to the second line of Eqn. 21 results in $a_{21} = 1/8$ and $a_{22} = 3/8$. Similarly, using $I(x, s) = \{1, x\}$ as the fitting functions to determine b in Eqn. 22 leads to

$$x_2 - x_0 = bx'|_{x_1} \tag{25}$$

then $b = 1$ is obtained.

Eqn. 25 has accuracy order of $O(x^2)$, while Eqns. 23-24 have accuracy order of $O(x^3)$. Therefore, the approximation frame in Eqns.21-22, which are determined by Eqns. 23-25, has compound order accuracy.

Substituting the coefficients into Eqn. 20, the four entries Y_{11}, Y_{12}, Y_{21} and Y_{22} have three common poles:

$$p_1 = -\frac{R}{L}$$

$$p_{2,3} = \frac{R}{2L}(-1 \pm \sqrt{1 - 32\frac{L}{R^2C}})$$

Accordingly, the residues of Y_{11} and Y_{22} are calculated as:

$$r_1 = \frac{1}{L}$$
$$r_{2,3} = \frac{\mp 32}{R\sqrt{R^2C^2 - 32LC} \pm (R^2C - 32L)}$$

and the residues of Y_{12} and Y_{21} are calculated as:

$$r_1 = -\frac{1}{L}$$
$$r_{2,3} = \frac{\mp 32}{R\sqrt{R^2C^2 - 32LC} \pm (R^2C - 32L)}$$

2.3 5th order poles

Select the value of N in Eqns. 9 and 10 to be 2, then along the line, five grid points are selected: $x_0 = 0$, $x_1 = 1/4$, $x_2 = 1/2$, $x_3 = 3/4$ and $x_4 = 1$. Following the process, four voltage variables $V_0 = V(x_0, s)$, $V_1 = V(x_1, s)$, $V_2 = V(x_3, s)$ and $V_3 = V(x_4, s)$, and three current variables $I_1 = I(x_0, s)$, $I_2 = I(x_2, s)$ and $I_3 = I(x_4, s)$ are selected. By applying the global approximation to compute the current and voltage difference, we obtain the following approximation frames:

$$\begin{bmatrix} V(x_1,s) - V(x_0,s) \\ V(x_3,s) - V(x_1,s) \\ V(x_4,s) - V(x_3,s) \end{bmatrix} = \begin{bmatrix} a_{11} & a_{12} & a_{13} \\ a_{21} & a_{22} & a_{23} \\ a_{31} & a_{32} & a_{33} \end{bmatrix} \begin{bmatrix} V'(x_0,s) \\ V'(x_2,s) \\ V'(x_4,s) \end{bmatrix} \quad (26)$$

and

$$\begin{bmatrix} I(x_2) - I(x_1) \\ I(x_3) - I(x_2) \end{bmatrix} = \begin{bmatrix} b_{11} & b_{12} \\ b_{21} & b_{22} \end{bmatrix} \begin{bmatrix} I'(x_1,s) \\ I'(x_3,s) \end{bmatrix} \quad (27)$$

where a_{ij} and b_{ij} are coefficients to be determined by using fitting functions. We choose $V(x, s) = \{1, x, x^2, x^3\}$ as the fitting functions to determine a_{21}, a_{22} and a_{23} (second line in Eqn. 26, that is

$$x_3 - x_1 = a_{21}x'|_{x_0} + a_{22}x'|_{x_2} + a_{23}x'|_{x_4} \quad (28)$$
$$x_3^2 - x_1^2 = a_{21}(x^2)'|_{x_0} + a_{22}(x^2)'|_{x_2} + a_{23}(x^2)'|_{x_4} \quad (29)$$
$$x_3^3 - x_1^3 = a_{21}(x^3)'|_{x_0} + a_{22}(x^3)'|_{x_2} + a_{23}(x^3)'|_{x_4} \quad (30)$$

which gives rise to $a_{21} = 1/48$, $a_{22} = 11/24$ and $a_{23} = 1/48$. To make the matrix A symmetric, set $a_{12} = a_{21}$ and $a_{13} = 0$. Using the fitting function $V(x, s) = \{1, x\}$ to determine the coefficients of the first line in Eqn. 26, we obtain $a_{11} = 11/48$. In the same way, we obtain $a_{31} = 0$, $a_{32} = 1/48$ and $a_{33} = 11/48$. The above process shows that the global approximations in Eqn. 26 have the accuracy order of $O(x^2)$ or $O(x^4)$.

Similarly, using $I(x, s) = \{1, x, x^2\}$ as the fitting functions to determine b_{ij} in Eqn. 27 obtains

$$x_2 - x_0 = b_{11}x'|_{x_1} + b_{12}x'|_{x_3}$$
$$x_2^2 - x_0^2 = b_{11}(x^2)'|_{x_1} + b_{12}(x^2)'|_{x_3}$$

then it follows $b_{11} = 1/2$ and $b_{12} = 0$, and similarly $b_{11} = 0$ and $b_{12} = 1/2$. The global approximations in Eqn. 27 have the accuracy order of $O(x^3)$.

Substituting the coefficients into Eqn. 20, the five common poles of the Y matrix are calculated as:

$$p_1 = -\frac{R}{L}$$
$$p_{2,3} = \frac{R}{2L}(-1 \pm \sqrt{1 - \frac{384}{11}\frac{L}{R^2C}})$$
$$p_{4,5} = \frac{R}{2L}(-1 \pm \sqrt{1 - \frac{384}{5}\frac{L}{R^2C}})$$

The corresponding residues for Y_{11} and Y_{22} are

$$r_1 = \frac{1}{L}$$
$$r_{2,3} = \frac{\mp 4608/11}{\sqrt{11}R\sqrt{11R^2C^2 - 384LC} \pm (11R^2C - 384L)}$$
$$r_{4,5} = \frac{\mp 1152/5}{\sqrt{5}R\sqrt{5R^2C^2 - 384LC} \pm (5R^2C - 384L)}$$

and the corresponding residues for Y_{12} and Y_{21} are

$$r_1 = -\frac{1}{L}$$
$$r_{2,3} = \frac{\mp 4608/11}{\sqrt{11}R\sqrt{11R^2C^2 - 384LC} \pm (11R^2C - 384L)}$$
$$r_{4,5} = \frac{\pm 1152/5}{\sqrt{5}R\sqrt{5R^2C^2 - 384LC} \pm (5R^2C - 384L)}$$

Higher order poles ($N > 2$) can be obtained by the similar way, in which the number of poles is $2N + 1$. However, as the order goes higher, the closed-form formula for the poles/residues become more complicated, which loses the simplicity and clarity. Therefore, the low order model is preferred. If the electrically long interconnect has to be handled, it can be divided into two or more separate interconnects, each of which can be modeled by the above low order pole modeling.

3 Companion models and passivity

The pole models can already be directly incorporated into the HSPICE, and it is significant that the pole-zero model runs much faster than other models [10]. However, there may be the trouble in this way that HSPICE cannot be able to find a DC path, which results in the simulation failure. On the other hand, companion models are better for transient simulation, which give the linear complexity with respect to the simulation time.

There are at least two approaches to transform the pole-residue models into the companion models. One is to use the Jordan-canonical form of realization which introduces new state variables [11], the other is to use the recursive convolution technique [8]. We choose to use the latter to obtain the companion models. While the detailed procedure to develop

the companion model is omitted in this paper, the resulted model is shown as in Fig. 3.

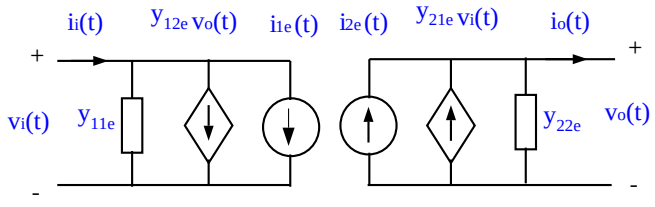

Figure 3: Companion model based on pole-residue modeling.

Passivity is a critical criteria for interconnect modeling. As stated in classical circuit theory, interconnections of stable systems may not necessarily be stable; interconnections of passive circuits are passive and therefore stable. When multiport models are connected together, the resulting overall circuit can guarantee to be stable only if each of the multiport models is passive [5]. In this view, it is extremely important to investigate the passivity of the presented methods. In order to do this, the following definitions and results are referred to [12].

(a) Necessary and sufficient conditions for a transfer function $n \times n$ matrix $Y(s)$ to be passive is that $Y(s)$ is positive-real: (i) each element of $Y(s)$ is analytic in $\Re(s) > 0$, (ii) $Y(s^*) = Y^*(s)$ and (iii) $(Y^*)^T(s) + Y(s)$ is non-negative definite for all $\Re(s) \geq 0$.

(b) An n-port network is passive if and only if its admittance matrix $Y(s)$ is positive-real.

(c) If $P(s)$ is positive-real, then $P^{-1}(s)$ is positive-real, if existed.

(d) If $P(s)$ is positive-real and B is real, then $B^T P(s) B$ is positive-real.

Substituting the different matrices A and B (as calculated in Section 2) into Eqn. 20 results in the Y matrices of the presented modeling approaches. Each of the Y matrices can be shown to be positive-real by the above lemmas, therefore the presented approaches maintain passivity.

The low order pole modeling can be straightforwardly extended to handle the multi-conductor transmission line (MTL). If an MTL contains m coupled interconnects, then the Y matrix represent a $2m$-port device, and the number of poles will increase by m times.

4 Numerical experiments

The *first* example is a single transmission line having the following PUL parameters: $l = 297\ nH/m$, $c = 144\ pF/m$ and $r = 193\ \Omega/m$. The interconnect length is $4\ cm$. By using the closed-form formula, the poles of the Y matrix are obtained, featuring 3rd, 5th and 7th orders. As comparison, the interconnect is segmented to 10 sections of lumped elements, which results in a Y matrix with 21 poles, as shown in Fig. 4.

Fig. 4 shows that all the poles are located on the negative half plane. The first poles calculated by the four approaches

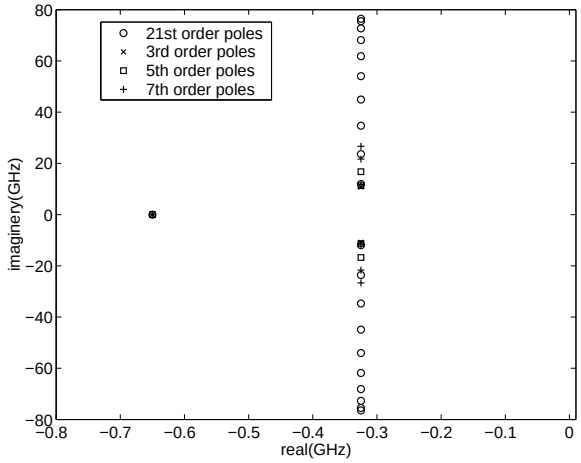

Figure 4: 3rd order, 5th order, 7th order poles and 21st order pole modeling.

are the same reals, the other conjugate pole pairs with same order differ to variant extent. Physically, the first poles (or pole pairs) are the most dominant poles, because they dominate the properties of the circuits. Further frequency analysis demonstrates that a small number of poles obtained from the presented methods retain high accuracy in a wide frequency range. Let the interconnect be excited by a pulse input with a internal inductance of $10\ nH$, and assume the load is a resistance of $50\ \Omega$. With the presented models being incorporated into HSPICE, the transient responses are calculated as shown in Fig. 5.

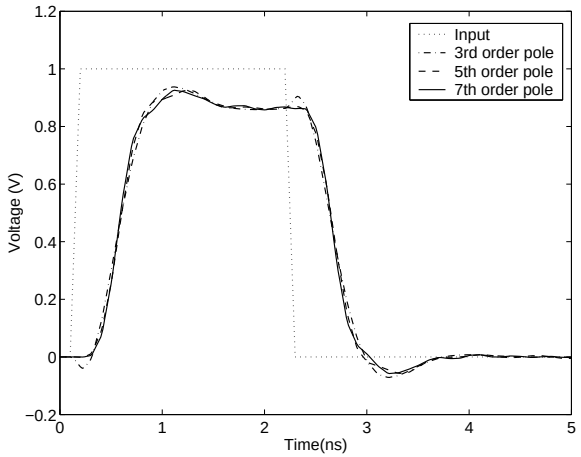

Figure 5: Transient responses of single transmission line.

The *second* example is a large linear network to further test the efficiency of the presented methods. The network is formed by cascading five identical cells, which are taken from [2]. Each of the cells includes seven different interconnects. The entire circuit has 35 interconnects and 92 nodes. The input excitations is a trapezoidal pulse with $0.1\ ns$ rise/fall

time and magnitude 1 V. We incorporate the companion models derived from the 3rd order pole and 5th order pole models into HSPICE frame, respectively. The transient waveforms are shown in Fig. 6, compared with the result of HSPICE discrete model. All the results agree so well that the difference is negligible.

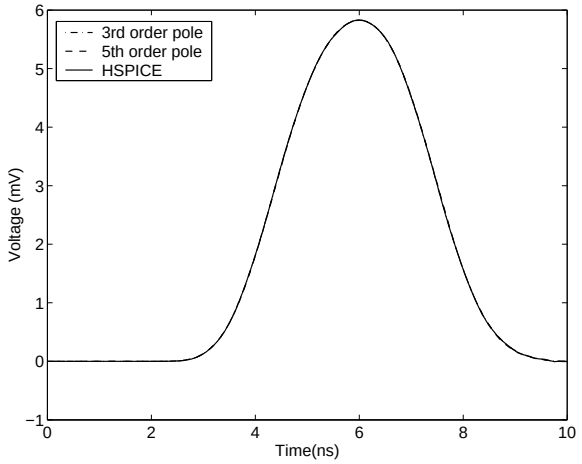

Figure 6: Transient responses of network containing 35 interconnects.

The performance data in solving the whole circuit of this example by the dominant pole modeling and by HSPICE are compared in Table 1. The presented methods are thrice faster than the U models of HSPICE.

Table 1: Comparison of pole modeling performance.

item	3rd order	5th order	HSPICE
Total memory (kB)	461	486	1180
Transient time (s)	0.72	0.86	2.43
Total CPU time (s)	1.44	1.40	4.30

5 Conclusions

The formulas to compute the low-order dominant poles for Y-matrix of interconnects are derived, and the companion models based on the reduced-order Y-matrix are obtained. By using the global approximation, the discrete approximation frameworks are constructed to transform the frequency-domain Telegrapher's equations into compact linear algebraic equations. Solving the linear equations, the closed-form formulas are obtained to calculate the low-order dominant poles. Due to high accuracy of the global approximation, the extracted poles can accurately represent the exact admittance matrices in a wide frequency range. By using the recursive convolution technique, the pole-residue models can be transformed into companion models, which have linear complexity with respect to the computational time. The presented modeling approaches are shown to preserve passivity. Numerical experiments of transient simulation demonstrate that the presented modeling approaches lead to higher efficiency, while maintaining comparable accuracy.

References

[1] L. T. Pillage and R. A. Rohrer, "Asymptotic waveform evaluation for timing analysis," *IEEE Trans. Computer-Aided Design*, vol. 9, no. 4, pp. 352–377, 1990.

[2] T. K. Tang and M. S. Nakhla, "Analysis of high-speed VLSI interconnect using the symptotic waveform evaluation technique," *IEEE Trans. Computer-Aided Design*, vol. 39, no. 3, pp. 341–352, 1992.

[3] E. Chiprout and M. S. Nakhla, "Analysis of interconnect networks using complex frequency hopping," *IEEE Trans. Computer-Aided Design*, vol. 14, no. 2, pp. 186–200, 1995.

[4] K. J. Kerns and A. T. Yang, "Stable and efficient reduction of large, multiport RC networks by pole analysis via congruence transformations," *IEEE Trans. Computer-Aided Design*, vol. 16, no. 7, pp. 734–744, 1997.

[5] A. Odabasioglu, M. Celik, and L. T. Pileggi, "PRIMA: Passive reduced-order interconnect macromodeling algorithm," *IEEE Trans Computer-Aided Design*, vol. 17, no. 8, pp. 645–653, 1998.

[6] R. Achar, P. K. Gunupudi, M. Nakhla, and E. Chiprout, "Passive interconnect reduction algorithm for distributed/measured networks," *IEEE Trans. circuits and systems II*, vol. 47, no. 4, pp. 287–301, 2000.

[7] D. B. Kuznetsov and J. E. Schutt-Aine, "Optimal transient simulation of transmission lines," *IEEE Trans. Circuits Syst. I*, vol. 43, no. 2, pp. 110–121, 1996.

[8] S. Lin and E. S. Kuh, "Transient Simulation of Lossy Interconnects Based on the Recursive Convolution Formulation," *IEEE Trans. Circuits and System*, vol. 39, no. 11, pp. 879–891, 1992.

[9] R. F. Harrington, *Field Computation by Moment Methods.* Macmillan, NY, 1962.

[10] Avant!, *Star-HSPICE Manual*. Avant! Corporation, 2000, 46871 Bayside Parkway, Fremont, CA 94538.

[11] R. Achar and M. S. Nakhla, "Simulation of high-speed interconnects," *Proceedings of the IEEE*, vol. 89, no. 5, pp. 693–728, 2001.

[12] R. W. Newcomb, *Linear Multiport Synthesis*. New York: McGraw Hill, 1966.